Deletion and anergy of polyclonal B cells specific for ubiquitous membrane-bound self-antigen

Justin J. Taylor,[2] Ryan J. Martinez,[1] Philip J. Titcombe,[1] Laura O. Barsness,[1] Stephanie R. Thomas,[1] Na Zhang,[1] Shoshana D. Katzman,[3] Marc K. Jenkins,[2] and Daniel L. Mueller[1]

[1]Department of Medicine and [2]Department of Microbiology, Center for Immunology, University of Minnesota Medical School, Minneapolis, MN 55455
[3]Department of Pathology, University of California San Francisco, San Francisco, CA 94143

B cell tolerance to self-antigen is critical to preventing antibody-mediated autoimmunity. Previous work using B cell antigen receptor transgenic animals suggested that self-antigen–specific B cells are either deleted from the repertoire, enter a state of diminished function termed anergy, or are ignorant to the presence of self-antigen. These mechanisms have not been assessed in a normal polyclonal repertoire because of an inability to detect rare antigen-specific B cells. Using a novel detection and enrichment strategy to assess polyclonal self-antigen–specific B cells, we find no evidence of deletion or anergy of cells specific for antigen not bound to membrane, and tolerance to these types of antigens appears to be largely maintained by the absence of T cell help. In contrast, a combination of deleting cells expressing receptors with high affinity for antigen with anergy of the undeleted lower affinity cells maintains tolerance to ubiquitous membrane-bound self-antigens.

CORRESPONDENCE
Daniel L. Mueller:
muell002@umn.edu

Abbreviations used: AF647, Alexa Fluor 647; APC, allophycocyanin; BCR, B cell receptor; DEL, duck egg lysozyme; FO, follicular; GPI, glucose-6-phosphate isomerase; HEL, hen egg lysozyme; MZ, marginal zone; Sm, smith antigen

Self-antigen–specific B cells are pathogenic in autoimmune diseases such as rheumatoid arthritis and systemic lupus erythematosus (Cohen et al., 2006; Mandik-Nayak et al., 2008; Shlomchik, 2008). It is not well understood how the mechanisms maintaining tolerance break down, resulting in the production of self-antigen–specific antibody. Antibody production in these situations is the result of the collaboration of two antigen-specific cell types: B cells, which differentiate into antibody-secreting cells, and $CD4^+$ helper T cells, which provide B cells with critical survival and differentiation signals (Seo et al., 2002).

What is known about B cell–intrinsic tolerance to self-antigen has been mostly determined using transgenic mice in which B cells express a B cell receptor (BCR) that is specific for self-antigen (Cambier et al., 2007; Shlomchik, 2008). These types of experiments have elegantly revealed two major mechanisms of tolerance within the B cell compartment. The first level of tolerance is a deletion of self-antigen–specific cells during development. This occurs through apoptosis of B cells expressing self-antigen–specific BCR (Nemazee and Bürki, 1989; Hartley et al., 1991) or through a process called receptor editing, which reduces BCR affinity for self-antigen (Gay et al., 1993; Tiegs et al., 1993). A second level of tolerance is a functional inactivation of cells termed anergy, which is thought to occur in cells that bind self-antigen but have escaped deletion (Goodnow et al., 1988). The contributions of deletion and anergy vary between the various BCR transgenic models (Cambier et al., 2007; Shlomchik, 2008). Consequently, the relative contributions that deletion and anergy play within the normal, nontransgenic population of self-antigen–specific B cells are unknown.

Recent investigation of BCRs cloned from individual human B cells suggest that as many as 20% of mature, naive B cells bear BCRs with a capacity to bind self-antigens (Meffre and Wardemann, 2008). Nevertheless, in most

The Rockefeller University Press $30.00
J. Exp. Med. 2012 Vol. 209 No. 11 2065-2077
www.jem.org/cgi/doi/10.1084/jem.20112272

individuals these self-reactive B cells cause no disease as a result of peripheral tolerance mechanisms. Such B cells are dangerous, however, as demonstrated in the glucose-6-phosphate isomerase (GPI) mouse model of arthritis. In this model, arthritis is caused by the production of antibodies specific for GPI, a ubiquitous self-protein found intracellularly and in serum (Kouskoff et al., 1996; Maccioni et al., 2002; Matsumoto et al., 1999, 2002). In this system, normal animals do not produce GPI-specific antibody until helper T cells specific for a GPI peptide are experimentally added (Kouskoff et al., 1996; Korganow et al., 1999; Maccioni et al., 2002; Matsumoto et al., 2002).

Although it is clear that self-antigen–specific B cells exist within a normal repertoire, the frequency and phenotype of such potentially pathogenic cells is unknown. To assess this, we adapted our recently published antigen-specific enrichment protocol (Pape et al., 2011) for use with nonfluorescent antigens. Using this approach, we analyzed B cells specific for GPI, as well as B cells specific for OVA, in WT and OVA-expressing mice. We report that a combination of deletion of BCR-expressing B cells with high affinity for self-antigen and of anergy of the remaining B cells expressing low-affinity BCR maintains tolerance to ubiquitous membrane-bound antigens. For GPI and other self-antigens not bound to membrane, deletion and B cell anergy do not appear to play a role. Instead, B cell tolerance to self-antigens not bound to membrane is maintained by the absence of T cell help.

RESULTS

Using antigen tetramers to analyze polyclonal antigen-specific B cells

The first step was to develop an antigenic tetramer reagent detectable by flow cytometry to ensure that low-affinity B cells would be identified. The tetramer consisted of an R-phycoerythrin (PE)–labeled streptavidin core and four biotinylated proteins. In Fig. 1, pooled spleen and LNs from WT mice were incubated with OVA-PE tetramer before enrichment using anti-PE magnetic microbeads. After enrichment, the bound fraction was labeled with a cocktail of B cell and non–B cell markers. Gating on B cells as immunoglobulin (Ig)$^+$ and CD8, CD4, Gr-1, CD11c, and F4/80 (non–B cells) that either expressed B220 or high levels of intracellular Ig (Fig. 1 A), a sizeable population of OVA tetramer–binding cells can be detected in the fraction that remained bound to the magnetized column (Fig. 1 B). However, the tetramer will bind not only B cells specific for OVA, but also B cells specific for PE, streptavidin (SA), and biotin epitopes within the tetramer. In fact, empty tetramers containing only PE, streptavidin, and biotin were

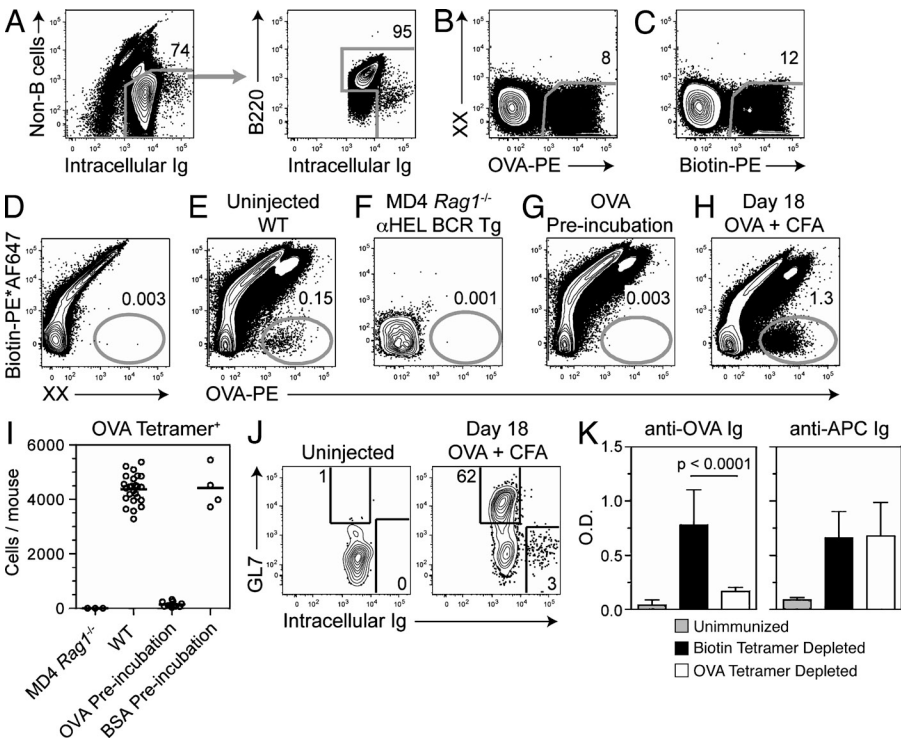

Figure 1. Analysis of OVA-specific B cells with an OVA tetramer. (A) B cells were identified by flow cytometry in pooled spleen and LN samples as cells that bound an antibody specific for Ig (binds both intracellular and surface Ig), but not a cocktail of antibodies specific for Thy1.2 (or CD4 and CD8), CD11c, Gr-1, or F4/80. Within the population, cells that neither expressed B220 or high levels of intracellular Ig were excluded. Representative flow cytometric analysis of gated B cells in a fraction enriched using anti-PE magnetic microbeads after staining with OVA-PE tetramer (B), Biotin-PE tetramer (C), Biotin-PE*AF647 tetramer (D), or both OVA-PE tetramer and Biotin-PE*AF647 tetramer (E–H). XX indicates an empty PE*AF647 (B and C) or PE (D) channel. In H, mice were injected s.c. with 1.4 nmol OVA emulsified in CFA 18 d before analysis. In G and I, cells were incubated with 300 µM of monomeric OVA or BSA beginning 20 min before tetramer labeling. (I) Combined data from 20 experiments showing the number of OVA tetramer$^+$ B cells in individual mice. The bar indicates mean. (J) Representative flow cytometric analysis of GL7 and intracellular Ig expression on gated OVA-specific B cells found in naive and mice injected s.c. with 1.4 nmol OVA emulsified in CFA. The flow cytometry plots shown in A–G and J are representative of at least three independent experiments. (K) Combined data from 2 experiments showing serum anti-OVA or anti-APC IgG+IgM measured 10 d after s.c. injection of *Rag1*$^{-/-}$ with 5.6 nmol of OVA and 0.1 nmol APC in CFA. Before injection, *Rag1*$^{-/-}$ received the entire fraction of spleen and LN cells that flowed through the column of a Biotin-PE*AF647 tetramer enrichment alone (Biotin tetramer depleted) or OVA-PE tetramer + Biotin-PE*AF647 tetramer enrichments (OVA tetramer depletion). Bars represent the mean ± SD (n = 5–9), and the p-value was established using an unpaired two-tailed Student's t test.

found to bind a number or B cells indistinguishable from OVA tetramers (Fig. 1 C). To gate out cells binding tetramer components, we conjugated Alexa Fluor (AF)647 to SA-PE loaded with biotin alone. The conjugation of AF647 to PE in this tetramer yields an emission transfer conjugate that can be clearly distinguished from PE (Fig. 1 D). This Biotin-PE*AF647 tetramer was preincubated with the sample before the addition of OVA-PE tetramer, and the sample was enriched with anti-PE microbeads. Using this strategy, most of the cells that bound the OVA-PE tetramer also bound the Biotin-PE*AF647 tetramer, whereas ∼4,000 cells bound only the OVA-PE tetramer (Fig. 1, E and I). OVA tetramer–binding was BCR-specific because few cells could be detected in MD4 *Rag1*$^{-/-}$ mice, which contain only B cells specific for hen egg lysozyme (HEL; Fig. 1, F and I). This BCR binding appeared OVA-specific because preincubation with a large molar excess of monomeric OVA, but not BSA, before OVA-PE incubation resulted in a loss of >98% of OVA tetramer–binding B cells (Fig. 1, G and I). Further demonstrating the OVA specificity of this population, the number of OVA tetramer–binding B cells expanded robustly after injection with OVA in CFA (Fig. 1 H). Within the expanded OVA-specific B cell population, GL7^{+} germinal center cells and intracellular Ig^{HI} antibody-secreting cells (plasma cell/blasts) were apparent after OVA injection (Fig. 1 J).

Although it was clear that OVA tetramers could detect OVA-specific B cells, it was unclear whether the ∼4,000 OVA tetramer–binding cells detected in uninjected animals represented the entire population of cells capable of responding to OVA injection. To assess this, we adoptively transferred the fraction of spleen and lymph node cells that was passed through the magnetized column (the tetramer-depleted fraction) into *Rag1*$^{-/-}$ recipients, which were subsequently injected s.c. with a high dose (5.5 nmol) of OVA in CFA. 10 d after injection, OVA-specific antibody produced by animals that received OVA tetramer–depleted cells was reduced by 80% compared with animals that received Biotin tetramer–depleted cells (Fig. 1 K). In contrast, the amount of antibody specific for a control antigen, allophycocyanin (APC), was not altered between the animals that received Biotin tetramer–depleted or OVA tetramer–depleted cells (Fig. 1 K). Thus, our enrichment procedure captures 80% of the cells capable of mounting an OVA-specific antibody response.

Enumerating OVA-specific B cells in OVA-expressing animals

We next assessed how the population of OVA-specific B cells would be affected when OVA was encountered as a self-antigen. In mice that ubiquitously secreted OVA (sOVA) under the control of the metallothionein promoter (Lohr et al., 2004), the number of OVA-specific B cells was not altered compared with WT counterparts (Fig. 2 A). In contrast, the OVA-specific B cell population was reduced by 40% in mice engineered to ubiquitously express membrane-bound OVA (mOVA) under the actin promoter (Fig. 2 B). This decrease was not the result of membrane-bound OVA blocking the binding of OVA tetramer during incubation, as mixing CD45.1^{+} WT and CD45.2^{+} mOVA samples before tetramer labeling did not alter the number of cells detected (unpublished data). We were concerned that this mixing experiment did not reflect the type of receptor down-regulation or receptor occupancy that could occur after exposure to membrane-bound OVA in vivo. To address this, we transferred CD45.1^{+} mature (AA4.1^{-}) WT B cells into CD45.2^{+} mOVA or WT recipients and found no difference in the number of OVA-specific WT donor cells recovered 7 d later (unpublished data). Together, these data indicate that the 40% decrease in OVA-specific B cells in mOVA mice occurs during development.

Naive peripheral B cells can be divided into three mature subsets (follicular [FO], marginal zone, and B1) and three immature (aka transitional) subsets (T1, T2, and T3) using flow cytometry. OVA-specific B cells found in WT mice were largely mature FO cells, with detectable numbers of marginal zone (MZ), B1, and transitional cells (Fig. 3, A and B). In mOVA mice, the number of FO and marginal zone B cells was reduced by ∼40%, whereas the small number of B1 cells was unaffected (Fig. 3 B). Within the immature transitional population, equal numbers of OVA-specific T1 cells were

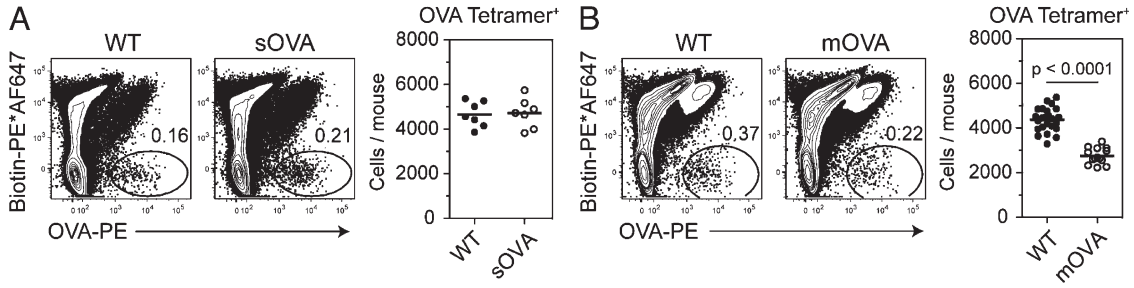

Figure 2. Enumeration of OVA-specific B cells in OVA-expressing animals. Representative flow cytometric analysis and total cell number of gated B cells in a fraction enriched using anti-PE magnetic microbeads after staining with both OVA-PE tetramer and Biotin-PE*AF647 tetramer from mice expressing secreted OVA (sOVA; A) or membrane-bound OVA (mOVA; B) mice. Corresponding WT mice are shown as a control. Data are combined from 7–15 experiments and represent the number of cells found in an individual mouse. The line indicates the mean (n = 7–26), and the p-value was established using an unpaired two-tailed Student's t test.

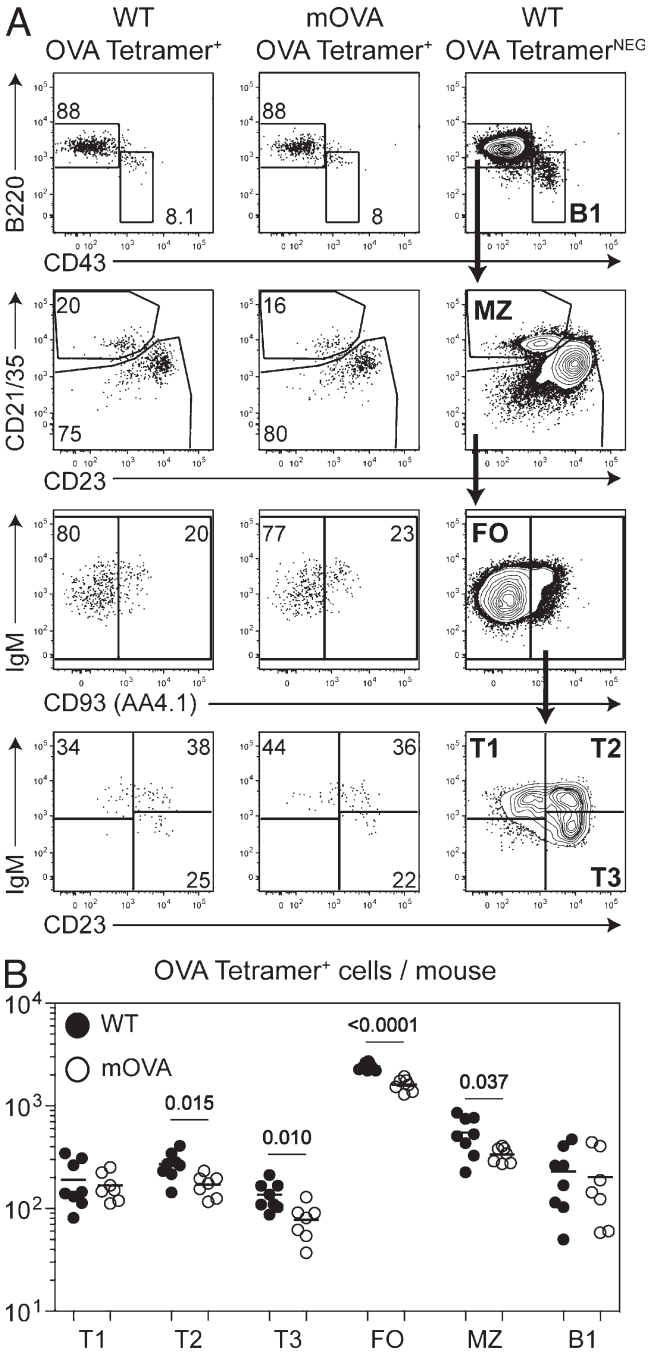

Figure 3. B cell subpopulation analysis of OVA-specific B cells from WT and mOVA-expressing animals. (A) Representative flow cytometric gating strategy for subpopulation analysis of OVA tetramer$^+$ and OVA Tetramer^{NEG} B cells (CD19$^+$ Thy1.2$^-$ CD11c$^-$ Gr-1$^-$ F4/80$^-$) in WT and mOVA mice. FO, mature FO; MZ, marginal zone. (B) Combined data from three experiments showing the total number of OVA tetramer$^+$ B cells within each subpopulation from individual mice ($n = 8$). The line indicates the mean, and the values above data points are p-values established using an unpaired two-tailed Student's *t* test.

detected in WT and mOVA mice (Fig. 3 B). In contrast, the number of T2 and T3 cells was significantly reduced in mOVA animals (Fig. 3 B). No difference in the number of OVA-specific B cells could be found within the immature B cell population found within the bone marrow (unpublished data). Collectively, the data indicate that the 40% reduction of OVA-specific B cells in mOVA mice occurs at the T1 to T2 transition, which has previously been shown to be a critical tolerance checkpoint where self-antigen–specific B cells are deleted from the repertoire (Meffre and Wardemann, 2008).

Measuring the median affinity of polyclonal OVA-specific B cells

The finding that only 40% of OVA-specific B cells were deleted from the OVA-specific repertoire was surprising given previous work demonstrating that cells expressing BCR specific for HEL are nearly completely deleted in mice that express membrane-bound HEL (Hartley et al., 1991). A potential explanation between our results and those published previously is that HEL-specific transgenic B cells are derived from post-germinal center cells that express a BCR with much higher affinity for HEL than would be expected for OVA-binding within a germline polyclonal repertoire. This idea is supported by other studies showing that cells expressing transgenic BCR with a high affinity for self-antigen are deleted, whereas cells expressing BCR with low affinity for the same self-antigen avoid deletion and remain functional (Wang and Shlomchik, 1997; Huang et al., 2006). Given these data, we hypothesized that within the 40% of OVA-specific B cells deleted in mOVA mice, cells express BCRs with the highest affinity for OVA. To test this, we developed a tetramer enrichment–based assay to measure the median affinity of the OVA-specific cells in WT and mOVA mice. In this assay, the sample was preincubated with increasing concentrations of monomeric protein before tetramer labeling and enrichment. The monomeric protein binds BCRs on the cells and blocks the binding of the tetramer and enrichment. Cells expressing BCRs with high affinity for antigen will bind monomeric protein when added at low concentrations, whereas cells with lower affinity BCRs will require high concentrations of protein to inhibit tetramer binding and enrichment. Thus, the concentration of protein required to inhibit the enrichment of 50% (IC_{50}) of the antigen-specific B cell population reveals the median affinity of the BCRs expressed by these cells.

We first assessed the validity of this assay using transgenic HEL-specific MD4 *Rag1*$^{-/-}$ B cells. MD4 B cells express a BCR that binds HEL with an exceptionally high affinity, and the related duck egg lysozyme (DEL), with >3,000-fold lower affinity (Lavoie et al., 1992). For this assay, we added ~4,000 transgenic HEL-specific MD4 B cells to a WT sample to approximate the number of OVA-specific B cells that we would ultimately assess. Samples were incubated with various concentrations of HEL, DEL, or OVA as a control for 20 min before DEL tetramer labeling and enrichment. In the enriched fractions, the number of IgM^{a+} DEL tetramer$^+$ MD4 cells (Fig. 4 A) was calculated and displayed as a percentage relative to samples that were incubated

without antigen (Fig. 4 B). MD4 cells do not bind OVA and correspondingly, 100% of the MD4 cells were enriched when samples were incubated with high concentrations of OVA (Fig. 4 B). In contrast, incubation with 5.3×10^{-12} M HEL or 10,000-fold more DEL (5.4×10^{-8} M) was required to reduce the number of enriched MD4 cells 50% (Fig. 4 B). This 10,000-fold increase in the concentration of DEL required for the inhibition of tetramer binding is consistent with the reported 3,000-fold lower affinity that the MD4 BCR has for DEL, indicating that the tetramer enrichment–based assay is capable of reporting differences in BCR affinity.

Using this assay, we found that a concentration of 3.1×10^{-6} M OVA was required to reduce the number of

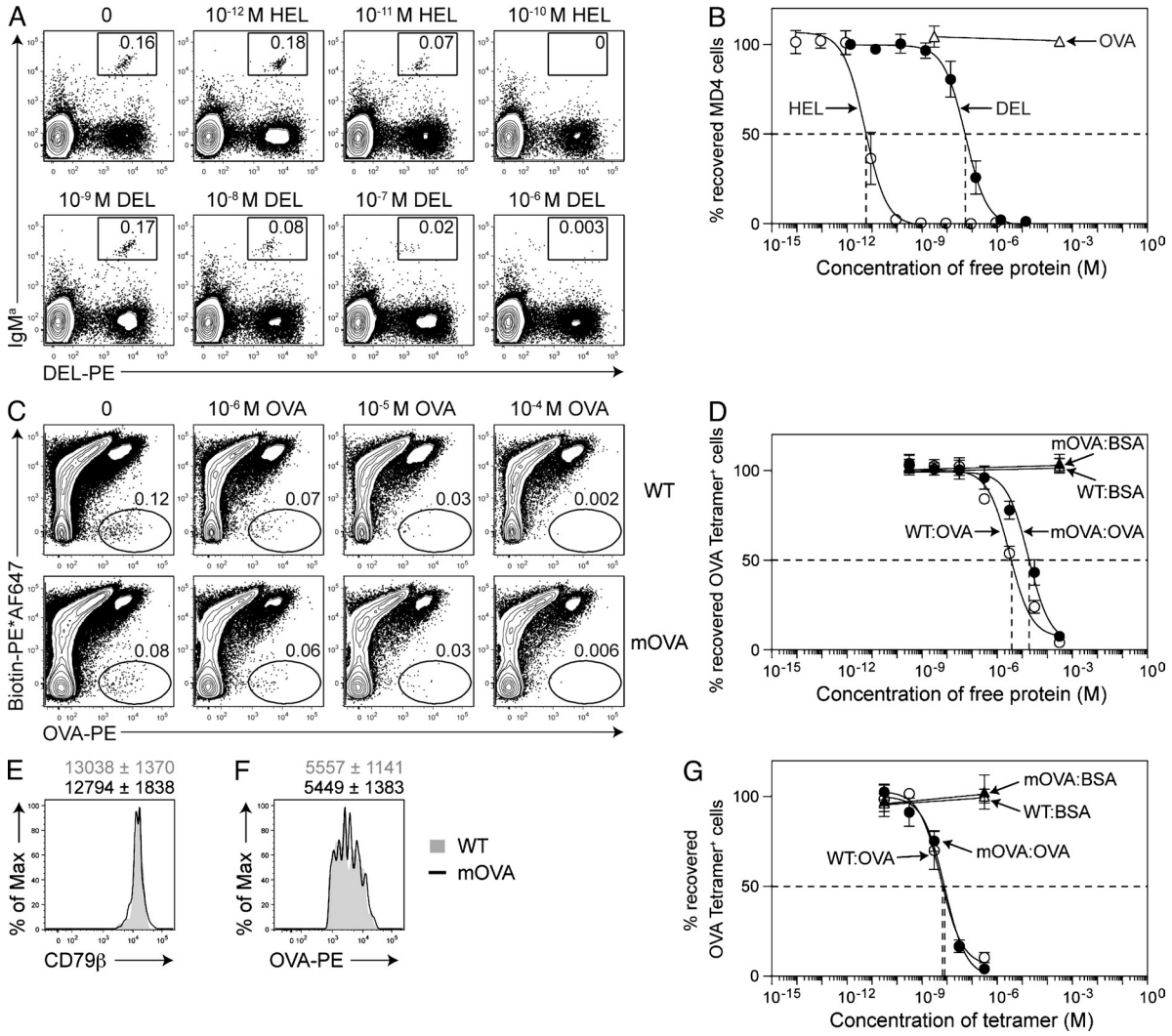

Figure 4. Measuring the median affinity of polyclonal OVA-specific B cells. Spleen and LNs from four mice were pooled and split equally into eight tubes and incubated with the noted concentration of monomeric antigen before tetramer enrichment and flow cytometric analysis. In A and B, ~16,000 MD4 *Rag1*$^{-/-}$ B cells were added to a WT B6 sample before antigen incubation (HEL, DEL, or OVA) and enriched using a DEL tetramer. (A) Representative flow cytometric analysis showing the detection of MD4 B cells as IgM^{a+} DEL tetramer^{+} cells. (B) Combined data from 6 experiments showing the percentage of MD4 cells recovered compared with the number of cells detected in a sample in which no monomeric antigen competitor was added. Each data point represents the mean ± SEM (n = 3–7). (C) Representative flow cytometric analysis showing the detection of OVA tetramer^{+} B cells from WT and mOVA mice with or without antigen (OVA or BSA) preincubation. (D) Combined data from three experiments showing the percentage of OVA tetramer^{+} B cells recovered compared with the number of cells detected in a sample in which no monomeric antigen competitor was added. Each data point represents the mean ± SEM (n = 3–7). (E) Representative flow cytometric analysis of surface Igβ (CD79b) expression by OVA Tetramer^{+} B cells from mOVA and WT mice. The numbers above the plots represent the mean fluorescence intensity ± SD (n = 5–6) of cells from individual WT (gray) and mOVA (black) animals from 2 experiments. (F) Representative flow cytometric analysis of the level of OVA tetramer^{+} on OVA tetramer^{+} B cells from mOVA and WT mice. Numbers above represent the mean fluorescence intensity ± SD (n = 11–12) of OVA tetramer from individual mice from 4 separate experiments. (G) Same as D, except samples were incubated with APC-conjugated OVA or BSA tetramers before labeling and enrichment with Biotin-PE*AF647 and OVA-PE tetramers. Each data point represents the mean ± SEM (n = 3).

OVA-specific WT B cells by 50% (Fig. 4, C and D). No decrease in OVA-specific B cells was found when samples were incubated with BSA as a control (Fig. 4 D). Compared with OVA-specific B cells from WT mice, a sixfold higher concentration of 1.7×10^{-5} M OVA was required to reduce the population of OVA-specific cells found in mOVA mice by 50% (Fig. 4 D). These differences in IC_{50} found for WT and mOVA mice were not a reflection of differences in BCR expression level, as both populations expressed similar levels of surface Igβ (Fig. 4 E). Furthermore, the presence of cells expressing membrane-bound OVA during the incubation period did not appear to influence this assay, as mixing CD45.1$^+$ WT and CD45.2$^+$ mOVA samples before antigen incubation and identification using congenic markers did not result in differences in the IC_{50} values for either population (unpublished data). These data indicate that OVA-specific B cells expressing BCRs with higher affinity for OVA are preferentially deleted in mice expressing membrane-bound OVA.

Despite the sixfold difference in median affinity, OVA-specific B cells from WT and mOVA mice bound similar levels of OVA tetramer (Fig. 4 F). This suggested that tetramerizing OVA negated the sixfold difference in affinity between WT and mOVA cells. Using the tetramer enrichment–based assay to measure avidity we found that, compared with OVA monomer, ~550-fold less OVA-tetramer (5.6×10^{-9} M) was required to reduce the population of OVA-specific cells found in WT animals by 50% (Fig. 4 G). Accounting for the 4 OVA molecules found in the tetramer, this represents a 140-fold increase in median affinity for individual OVA molecules. Consistent with the level of tetramer binding, OVA-specific B cells from mOVA mice exhibited an affinity for OVA tetramer (7.9×10^{-9} M) that was similar to that of WT cells (Fig. 4 G).

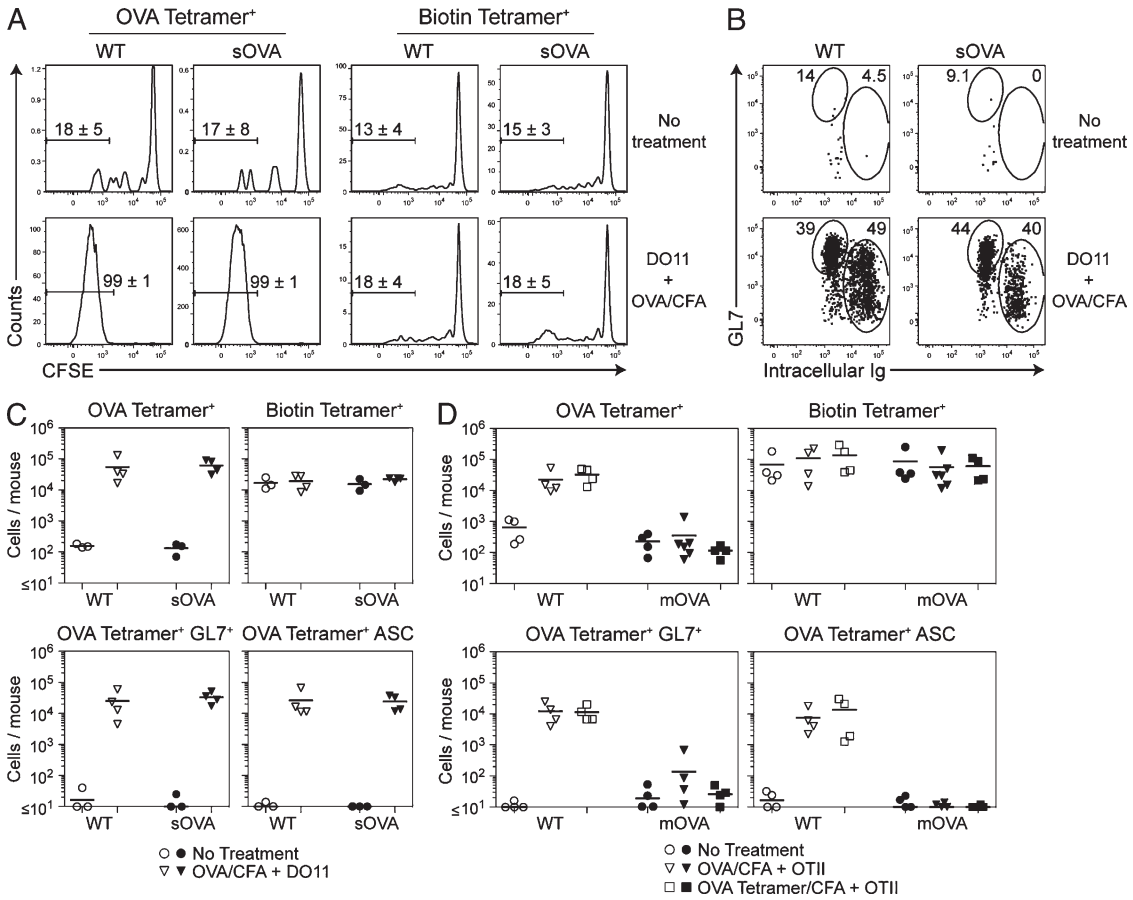

Figure 5. Functional capabilities of OVA-specific B cells found in OVA-expressing animals. MACS-purified B cells from sOVA, mOVA, or WT control mice were CFSE-labeled and adoptively transferred into *Rag1*$^{-/-}$ recipients. Some mice also received 10,000 syngeneic OVA-specific CD4$^+$ helper T cells (DO11 *Rag2*$^{-/-}$ or OTII *Rag1*$^{-/-}$) and s.c. injection of 5.5 nmol of OVA or 1.4 nmol OVA tetramer in CFA 7 d before analysis. After OVA-PE tetramer and Biotin-PE*AF647 tetramer labeling and enrichment, gated OVA tetramer$^+$ and Biotin tetramer$^+$ cells were analyzed for CFSE dilution (A) or GL7 and intracellular Ig expression (B). Representative plots are shown and the numbers represent the mean ± SD (n = 3–4) percentage of CFSE^{LOW} cells found in individual mice from 2 combined experiments. Combined data from three to four experiments showing the total number of OVA tetramer$^+$, Biotin tetramer$^+$, OVA tetramer$^+$ GL7$^+$, and OVA tetramer$^+$ ASC (Ig^{HI}) B cells in individual recipients of sOVA (C) or mOVA (D) B cells. Corresponding WT mice are shown as a control. The line indicates the mean (n = 3–6).

Examining the function of OVA-specific B cells from OVA-expressing animals

To examine the function of OVA-specific B cells present in OVA-expressing mice, we purified B cells from WT or OVA-expressing mice and adoptively transferred them into *Rag1*$^{-/-}$ recipients. T cells that expressed a TCR specific for OVA were co-transferred, and the recipient mice were subsequently injected with a high dose of OVA (5.4 nmol) in CFA. This adoptive transfer approach was designed to normalize the amount of antigen and CD4^{+} help provided to the OVA-specific B cell populations from WT and OVA-expressing mice. Further, we transferred total B cells instead of purified OVA-specific B cells to avoid potential artifacts resulting from BCR being stimulated by the OVA tetramers that would have been coated on the cells at the time of adoptive transfer. In the absence of stimulation, little proliferation or differentiation could be found within the OVA-specific population 7 d after transfer (Fig. 5 A). In contrast, 7 d after the injection of OVA in CFA and DO11 T cells, OVA-specific B cells from WT and sOVA mice proliferated (Fig. 5, A and C) and differentiated (Fig. 5, B and C) equivalently. This response was not the result of nonspecific stimuli because the population of cells binding the biotin tetramer did not proliferate in response to OVA injection (Fig. 5, A and C). In contrast to the response of cells from sOVA mice, OVA-specific B cells from mOVA mice did not proliferate or differentiate in response to OVA in CFA injection (Fig. 5 D).

In Fig. 4, we showed that the median affinity of OVA-specific B cells from mOVA mice was sixfold lower than OVA-specific B cells found in WT animals. Given this data, we considered whether the inability of OVA-specific B cells from mOVA mice to respond to OVA injection was a result of these cells exhibiting an affinity for OVA too low to respond to OVA in CFA. To test this idea, we injected mice with OVA tetramer in CFA, which binds OVA-specific cells in WT and mOVA cells with a similarly high avidity (Fig. 4). Despite this high avidity, OVA-specific cells from mOVA mice did not respond to injection with OVA tetramer in CFA (Fig. 5 D). Thus, the OVA-specific B cells that escape deletion in the mOVA animal respond poorly to OVA, whereas those found in sOVA mice have normal function.

The inability to respond to OVA tetramer priming suggested that OVA-specific B cells from mOVA mice were anergic. Despite this functional unresponsiveness, OVA-specific B cells from mOVA were indistinguishable from the functional naive OVA-specific B cells from WT mice based on the expression of CD24 (HSA), CD38, CD40, CD44, CD80, CD86, CD95 (FAS), IgD, IgM, and MHCII (Fig. 6). Given this naive phenotype, we were concerned that our in vivo priming experiments may not accurately reflect the function of OVA-specific B cells from mOVA mice. For example, if the OVA tetramer was not stable in vivo, then B cells would actually be encountering monomeric protein. Therefore, we analyzed the proliferation of OVA-specific B cells providing polyclonal stimulation in vitro. In these assays, total B cells were plated and stimulated for 72 h with anti-IgM and anti-CD40 before enrichment with OVA tetramers. OVA-specific B cells from mOVA animals proliferated normally in response to anti-CD40 stimulation alone, but responded poorly when BCR was stimulated with anti-IgM (Fig. 7). This poor response was confined to the OVA-specific B cells because B cells binding the biotin tetramer within the same culture responded normally to anti-CD40 and anti-IgM stimulation (Fig. 7). Thus, the OVA-specific B cells that escape deletion in the mOVA animal are functionally anergic to BCR stimulation.

Analysis of GPI-specific B cells

Because the natural self-antigen GPI is not membrane-bound, we hypothesized that GPI-specific B cells would resemble OVA-specific B cells in sOVA mice. To assess the number and function of GPI-specific B cells, we generated a GPI-PE tetramer as well as PE*AF647 tetramer containing a poly-HIS tagged irrelevant protein (C5a peptidase from Group A Streptococcus).

After tetramer labeling and enrichment, ~6,700 B cells bound the GPI-PE tetramer, but not the C5a-PE*AF647 tetramer, whereas few GPI tetramer-binding cells could be detected in the HEL-specific B cell population of MD4 *Rag1*$^{-/-}$ mice (Fig. 8, A and B). Similar

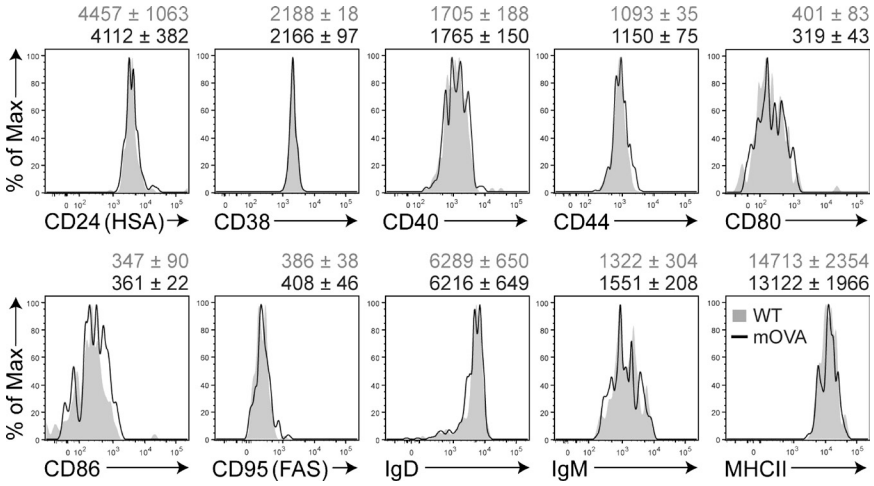

Figure 6. Surface marker expression by OVA-specific B cells found in mOVA-expressing animals. Representative flow cytometric analysis of the expression of MHC class II (MHCII), CD95 (FAS), CD38, CD40, CD44, CD80, CD86, CD24 (HSA), IgM, and IgD by mature FO OVA tetramer^{+} B cells from mOVA and WT mice gated as shown in Fig. 3. The numbers above the plots represent the mean fluorescence intensity ± SD (n = 3–8) from individual WT (gray) and mOVA (black) animals combined from 2–4 experiments per marker.

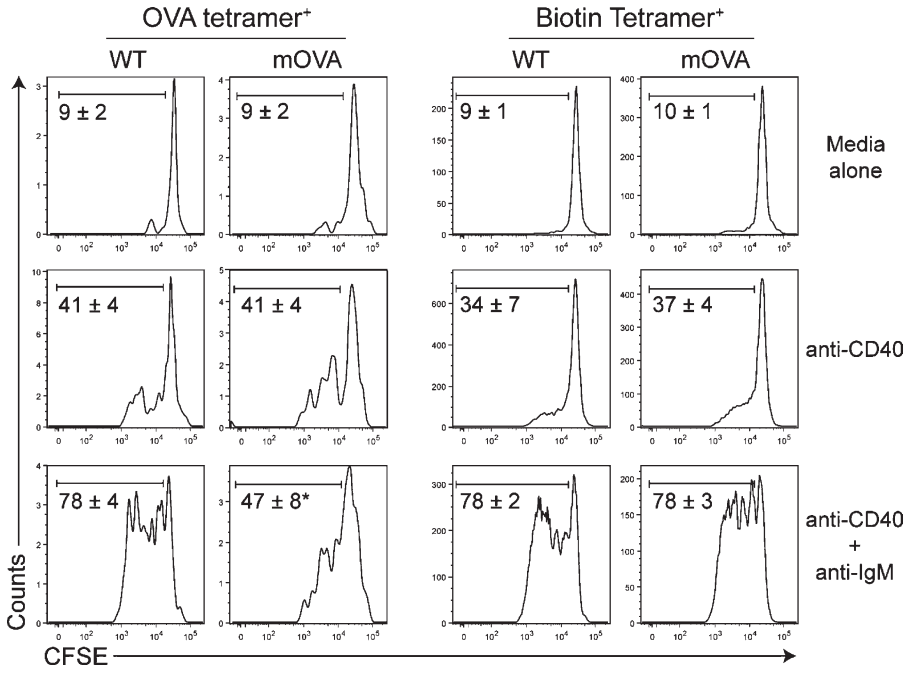

Figure 7. In vitro response of OVA-specific B cells from WT and mOVA-expressing animals. MACS-purified B cells from mOVA or WT control mice were cultured in vitro in the presence of 1 µg/ml αCD40, 1 µg/ml αCD40, and 5 µg/ml αIgM, or media alone for 72 h before tetramer labeling and enrichment and analysis of CFSE dilution. The numbers on the plot represent the mean percentage (±SD) of $CFSE^{LOW}$ cells found in three separate experiments. *, P = 0.038 compared with the percentage of $CFSE^{LOW}$ cells found in the OVA tetramer+ population from WT mice stimulated with αCD40 and αIgM.

to OVA-specific B cells in normal mice, the majority of the GPI-specific B cells were mature FO cells, with detectable numbers of transitional, marginal zone and B1 cells (Fig. 8 C). Analysis of median affinity of the population revealed that the GPI-specific B cell population had an IC_{50} of 2.2×10^{-5} M (Fig. 8 D).

To test the function of GPI-specific B cells, we adoptively transferred KRN transgenic $CD4^+$ helper T cells, which are specific for a GPI peptide bound to $I\text{-}A^{g7}$, into *Tcra*$^{-/-}$ B6.I-$A^{b/g7}$ recipients (Korganow et al., 1999; Martinez et al., 2012). In this system, recipient mice develop arthritis mediated by GPI-specific IgG1 (Maccioni et al., 2002) beginning at day 7 or 8 (Fig. 8 E). Correspondingly, a robust expansion of GPI-specific B cells was detected 7 d after adoptive transfer of KRN T cells into *Tcra*$^{-/-}$ B6.I-$A^{b/g7}$ recipients (Fig. 8, A and B). The expanded GPI-specific population found 7 d after KRN transfer contained both $GL7^+$ germinal center cells and intracellular Ig^{HI} antibody-secreting cells (Fig. 8 F). Additionally, more than half of the $GL7^+$ and intracellular Ig^{HI} cells expressed IgG1 BCR heavy chains 7 d after KRN transfer (Fig. 8 G).

We next assessed whether the GPI tetramer-binding B cells found in naive animals were truly the B cells responsible for the induction of arthritis after KRN T cell transfer. To do this we adoptively transferred FACS-purified GPI tetramer-binding B cells into NOD *Rag1*$^{-/-}$ *IL2rγ*$^{-/-}$ recipient mice. These recipients were used because they express $I\text{-}A^{g7}$ and lack T cells, B cells, and NK cells that could potentially reject the transferred T and B cells, which are on a B6 $I\text{-}A^{b/g7}$ background. 12 d after the transfer of KRN T cells, arthritis could be detected in most of the recipients of GPI tetramer-binding B cells, but not the control recipients that received B cells that bound the C5a tetramer (Fig. 8 G). The arthritis scores found in these experiments varied greatly between individual animals but correlated strongly with the number of GPI-specific B cells that could be detected in the animal (Fig. 8 I). Few, if any, GPI tetramer-binding B cells could be found in the recipients of C5a tetramer-binding B cells (unpublished data). Thus, from our data it is clear that naive GPI-specific B cells are present and functional despite GPI being a ubiquitous self-antigen found in serum.

DISCUSSION

Our characterization of GPI-specific polyclonal B cells, together with the data generated from sOVA mice, indicates that tolerance to self-antigens found in serum is mainly B cell extrinsic, as deletion and anergy were undetectable in these systems. B cell tolerance to these self-antigens relies mainly on a lack of T cell help, perhaps through the deletion of self-antigen–specific helper T cells during development, helper T cell anergy, or the activity of regulatory T cells.

Data from several BCR transgenic models has shown that deletion is an important mechanism of B cell tolerance. Here, we have extended these findings by looking for deletion in an endogenous population. Within the endogenous population, we detect deletion of OVA-specific B cells in animals that ubiquitously express mOVA. Not surprisingly, the cells deleted from the repertoire are those that have higher affinity for OVA compared with their undeleted counterparts. In WT mice, OVA-specific B cells express receptors that have a median affinity that is 600,000-fold less than the affinity of the MD4 BCR for HEL. In mOVA mice, the 60% of cells that are not deleted have a median affinity for OVA that is ~3,400,000-fold lower than the MD4 BCR for HEL. From these results, we conclude that MD4 cells are completely deleted from mice that expressed membrane-bound HEL because the affinity of the MD4 BCR far exceeds the threshold necessary for deletion. Because the median BCR affinity of the cells remaining in the mOVA mice are >300-fold less

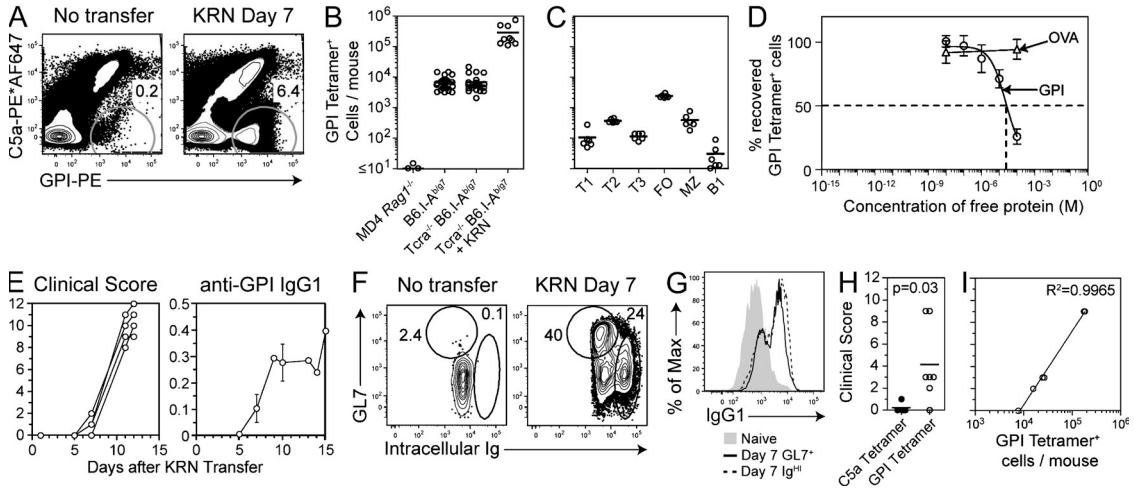

Figure 8. Analysis of GPI-specific B cells in an adoptive transfer model of arthritis. (A) Representative flow cytometric analysis from 15 experiments of gated B cells in the GPI-PE tetramer and C5a-PE*AF647 tetramer-enriched fraction of *Tcra*$^{-/-}$ B6.I-A$^{b/g7}$ mice with and without adoptive transfer of GPI-specific CD4$^+$ helper T cells (KRN) 7 d before analysis. (B) Combined data from 15 experiments showing the number of GPI tetramer$^+$ B cells in individual HEL-specific MD4 *Rag1*$^{-/-}$, B6.I-A$^{b/g7}$, *Tcra*$^{-/-}$ B6.I-A$^{b/g7}$, and *Tcra*$^{-/-}$ B6.I-A$^{b/g7}$ mice 7 d after transfer of KRN cells. The line indicates the mean (n = 3–26). (C) Combined data from three experiments showing the number of GPI tetramer$^+$ B cells of each subpopulation identified as shown in Fig. 3. (D) Combined data from four experiments showing the percentage of GPI Tetramer$^+$ B cells recovered in the presence of monomeric GPI or OVA competitor as compared with the number of cells detected in a sample in which no competitor antigen was added. Each data point represents the mean ± SEM (n = 5). (E, left) Pooled data from 2 experiments showing the arthritis clinical disease activity scores (max = 12) of individual *Tcra*$^{-/-}$ B6.I-A$^{b/g7}$ mice (n = 4) and (right) mean (n = 5; ± SEM) serum anti-GPI IgG1 measured on the days indicated after adoptive transfer of KRN CD4$^+$ helper T cells. Serum anti-GPI IgG1 antibody levels reflect the optical density measured at 1:900 dilution of serum. (F) Representative flow cytometric analysis from 5 experiments showing GL7 and intracellular Ig expression on gated GPI tetramer$^+$ B cells 7 d after transfer of KRN cells. (G) Representative flow cytometric analysis from 3 experiments showing surface IgG1 expression on GL7$^+$ and intracellular Ig^{HI} GPI tetramer$^+$ populations 7 d after transfer of KRN cells. (H) Pooled data from 3 experiments showing the arthritis clinical disease activity scores (max = 12) 12 d after the transfer of KRN CD4$^+$ helper T cells into NOD *Rag1*$^{-/-}$ *IL2rγ*$^{-/-}$ recipient mice that received FACS-purified GPI tetramer$^+$ or C5a tetramer$^+$ B cells. Each data point indicates an individual mouse (n = 5–7), and the bar indicates the mean. The p-values were established using an unpaired two-tailed Student's t test. (I) Arthritis clinical disease activity scores from the recipients of GPI tetramer$^+$ B cells from H plotted against the total number of GPI tetramer$^+$ B cells in the recipient animals 12 d after the transfer of KRN CD4$^+$ helper T cells.

than the affinity of the MD4 BCR for DEL, we predict that if mice expressing membrane-bound DEL were generated, MD4 cells would also be deleted in these animals.

Based on data from knock-in animals expressing GPI-specific BCR heavy and light chain genes, B cells expressing a somatically hypermutated BCR with high affinity for GPI arrest in the transitional stage and are later deleted from the repertoire, whereas those expressing BCR with lower affinity for GPI avoid deletion and mature normally (Huang et al., 2006). Because GPI-deficient animals are not viable, we cannot directly gauge the effect that deletion might have upon the endogenous GPI-specific B cell population. The median affinity of the GPI-specific B cell population was similar to the OVA-specific B cell population remaining in mOVA animals, which could be consistent with deletion of clones with high affinity for GPI. However, if deletion of B cells expressing germline encoded GPI-specific BCRs does occur, it is clearly inefficient, as the frequency of GPI-specific B cells is higher than the frequency of naive B cells specific for foreign antigens such as OVA (Fig. 1) or APC (Pape et al., 2011) in WT uninjected mice.

The robust T cell–driven responses of both GPI-specific B cells and OVA-specific B cells in sOVA mice were initially surprising in light of the data generated in mice expressing soluble HEL and transgenic MD4 BCR (Goodnow et al., 1988). In these studies, functional anergy could be detected in animals where the serum level of HEL reached 0.1 nM (Adelstein et al., 1991), a concentration exceeded by GPI in WT mice (5 nM; Matsumoto et al., 2002) and OVA in sOVA animals (0.2 nM; Abbas et al., 2007). An explanation for these differences is that MD4 B cells are derived from post-germinal center cells that express a BCR that has a 600,000-fold higher affinity for HEL than the median BCR affinity for GPI or OVA. It is intriguing to speculate that anergy within the OVA-specific population could be achieved if the level of soluble OVA was increased by 600,000-fold to account for the lower BCR affinity. Alternatively, anergy might also be attainable if OVA was presented in multimeric form like many clinically relevant soluble antigens. If OVA were present in serum in tetramerized form, which OVA-specific cells can bind with a 550-fold increased affinity, only a 1,000-fold increase in concentration may be required to achieve anergy.

Collectively, our work indicates that anergy is an important tolerance mechanism for B cells that are specific for ubiquitous membrane-bound self-antigens that survive beyond the T1 to T2 self-tolerance checkpoint (Meffre and Wardemann, 2008). Consistent with this model, anergy can be seen in the membrane-bound HEL system when MD4 cells survive as a result of forced Bcl-XL expression (Fang et al., 1998). In some systems, anergic B cells have often been found to express the T3 ($CD93^+$ $CD23^+$ IgM^{LO}) phenotype (Merrell et al., 2006; Cambier et al., 2007). However, the number of OVA-specific T3 cells in mOVA mice was reduced compared with WT mice. Instead, the anergic OVA-specific B cells in mOVA animals resemble the non-T3 anergic B cells that have been described in other systems (Cambier et al., 2007).

The rules governing whether an anergic B cell will exhibit a T3 or non-T3 phenotype are not well understood. One explanation is that it varies based on the expression level or cellular distribution of the different self-antigens. However, the control of anergic B cell phenotype is clearly more complex given that Smith antigen (Sm)-specific polyclonal B cells are enriched within the T3 anergic population of normal mice, whereas anergic BCR transgenic anti-Sm B cells do not express the T3 phenotype (Borrero and Clarke, 2002; Merrell et al., 2006). One of these studies (Borrero and Clarke, 2002) noted an increase in the expression of MHCII and CD95 (FAS) on anergic cells, but these proteins were not differentially expressed by mature FO OVA-specific B cells in WT and mOVA mice. Likewise, the expression of CD24 (HSA), CD38, CD40, CD44, CD80 and CD86 were also similar between mature FO OVA-specific B cells in WT and mOVA mice. Thus, OVA-specific B cells found in mOVA mice appear phenotypically naive despite their functional anergy. Future work will be aimed at finding markers capable of differentiating between naive and anergic B cells so that we can begin to assess what fraction of the mature peripheral B cell population is truly naive.

In humans, anergic B cells have been identified as exhibiting an IgD^{HI} IgM^{LO} phenotype (Duty et al., 2009; Quách et al., 2011). In contrast, OVA-specific B cells found in WT and mOVA mice expressed high levels of both IgD and IgM. This indicates that either the non-T3 anergic phenotype does not translate into humans, or anergic human B cells are not limited to the IgD^{HI} IgM^{LO} compartment. The only way to distinguish between these two possibilities is to directly phenotype human B cells that are specific for self-antigens. The enrichment and detection strategy described herein is translatable for use with human samples, and should allow for the investigation of self-antigen–specific B cells in both healthy and autoimmune individuals.

There are some notable limitations of our work that may be able to be improved in future studies. One limitation is that we are unable to subdivide cells with different affinities for antigen and, instead, assess all cells with an affinity capable of binding tetramerized antigen. This limitation prevents us from saying that there is a complete lack of deletion or anergy within the population of OVA-specific B cells in sOVA animals. For example, if deletion or anergy occurred in the 2% of cells demonstrating the highest affinity for OVA in the sOVA animal, we would not be able to detect this loss. However, if this occurs in sOVA animals, these mechanisms are clearly inefficient because functional OVA-specific B cells remained and responded robustly when antigen and T cell help was provided. Likewise, if 2% of the OVA-specific B cell population in the mOVA mouse were deleted in the bone marrow, we would be unable to detect this small loss. Our attempts to focus only on the highest affinity B cells through the use of monomeric detection reagents have been unable to reliably detect cells. Perhaps future studies using antigen dimers or trimers will be able to focus specifically on high-affinity B cells.

A second limitation to our work is that we can only assess B cells with high enough affinity to bind the tetramer. This could be important in the mOVA animal, where it is possible that some B cells have too low an affinity for OVA to bind the tetramer but have a high enough affinity for OVA to be rendered anergic when they encounter membrane-bound OVA in the animal. Future work with further multimerization could address this issue.

MATERIALS AND METHODS

Animals. 6–10-wk-old, sex-matched mice were used for experiments. C57BL/6 (B6) mice, B6.CD45.1 congenic (B6.SJL-*Ptprca Pep3b*/BoyJ), and BALB/c mice were purchased from the National Cancer Institute (Frederick, MD). DO11.10 *Rag2*$^{-/-}$ mice were purchased from Taconic. BALB/c *Rag1*$^{-/-}$ (C.129S7(B6)-Rag1^{tm1Mom}/J) and B6 *Tcra*$^{-/-}$ (B6.129S2Tcra^{tm1Mom}/J) mice were purchased from The Jackson Laboratory. NOD *Rag1*$^{-/-}$ *IL2rγ*$^{-/-}$ mice were purchased from The Jackson Laboratory and provided by B. Fife (University of Minnesota, Minneapolis, MN). KRN (Kouskoff et al., 1996), B6.I-A^{g7} (Kouskoff et al., 1996), B6.I-A^{g7} *Tcra*$^{-/-}$, B6.I-A^{b} *Tcra*$^{-/-}$, B6 *Rag1*$^{-/-}$ (Mombaerts et al., 1992), OTII (Barnden et al., 1998) *Rag1*$^{-/-}$, and MD4 (Goodnow et al., 1988) *Rag1*$^{-/-}$ mice were maintained in-house. B6.I-$A^{b/g7}$ and B6.I-$A^{b/g7}$ *Tcra*$^{-/-}$ were the offspring of B6.I-A^{b} x B6.I-A^{g7} and B6.I-A^{b} *Tcra*$^{-/-}$ x B6.I-A^{g7} *Tcra*$^{-/-}$ crosses, respectively. Act-2W-mOVA mice were described previously (Moon et al., 2011), and surface expression of OVA was confirmed by flow cytometry. All of the aforementioned mice were maintained in a specific pathogen–free facility under protocols approved by the University of Minnesota Institutional Animal Care and Use Committee and in accordance with National Institutes of Health (NIH) guidelines. sOVA mice were generated as previously described (Lohr et al., 2004) and maintained in specific pathogen–free facility with protocols approved by the Laboratory Animal Resource Center of the University of California San Francisco in accordance with NIH guidelines.

Tetramer production. Recombinant protein (GPI or truncated C5a peptidase) was expressed and produced by *Escherichia coli* (provided by H. Huang [University of Chicago, Chicago, IL] and P. Cleary [The University of Minnesota, Minneapolis, MN], respectively). Transfected *E. coli* bacteria were selected in carbenicilin or kanamycin containing medium overnight at 37°C, and then passaged to cultures at 1:200 and incubated for 3–4 h (37°C). Isopropyl β-D-1-thiogalactopyranoside (Sigma-Aldrich) was added to cultures, and cultures were incubated overnight at 37°C. GPI or C5a peptidase was purified using a His-Bind purification kit (EMD Chemicals). Purified protein was separated from *E. coli* proteins using a Sephacryl S-300 size exclusion column (GE Healthcare). OVA and BSA were purchased from Sigma-Aldrich, HEL was purchased from Biozyme Laboratories, and DEL was obtained by special order from Worthington Biochemical Corporation.

Molar concentration was confirmed/determined by measuring the absorbance at 280 nM using a NanoDrop (Thermo Fisher Scientific). Extinction coefficients used were as follows: OVA = 0.0269 $cm^{-1}\mu M^{-1}$; BSA = 0.0438 $cm^{-1}\mu M^{-1}$; HEL = 0.0376 $cm^{-1}\mu M^{-1}$; DEL = 0.0408 $cm^{-1}\mu M^{-1}$; GPI = 0.0838 $cm^{-1}\mu M^{-1}$.

Purified protein was biotinylated using an EZ-link Sulfo-NHS-LC-Biotinylation kit (Thermo Fisher Scientific) using a 1:1 ratio of biotin to protein. Desalting columns (GE Healthcare) were used to remove free biotin. The molar amount of biotinylated protein was measured using a Western blot. In brief, biotinylated target protein was held at a constant concentration, and differing amounts of SA-PE (ProZyme) were titrated in and incubated at room temperature. Samples were then loaded and ran on a SDS-Page gel (Bio-Rad Laboratories). The gel was transferred to nitrocellulose and probed with SA-AF680 (Invitrogen) to determine the point at which there was excess biotin available for the SA-AF680 reagent to bind. This ratio was then used to calculate the concentration of biotinylated target protein, and the amount of SA-PE or SA-APC (ProZyme) to add to create a 6:1 ratio of target protein/SA-PE. Biotinylated protein were mixed with SA-PE for 30 min at room temperature and purified on a Sephacryl S-300 size exclusion column. The tetramer fraction was centrifuged in a 100-kD molecular weight cutoff Amicon Ultra filter (Millipore). Because the ratio of SA/fluorochrome is roughly 1:1, the concentration of tetramer was calculated by measuring the absorbance of PE at 565 nM (extinction coefficient = 1.96 $cm^{-1}\mu M^{-1}$) or APC at 650 nM (extinction coefficient = 0.7 $cm^{-1}\mu M^{-1}$). The tetramer was stored at a concentration of 1 µM.

The nonspecific tetramer was created in-house in the same fashion as the OVA and GPI tetramers, but for the C5a peptidase and biotin tetramer, the core fluorochrome was SA-PE conjugated to AF647 (Invitrogen) for 60 min at room temperature. The free AF647 that was removed by centrifugation in a 100-kD molecular weight cut off Amicon Ultra filter (Millipore). The SA-PE*AF647 complex concentration was calculated by measuring the absorbance of PE at 565 nm, and the solution was brought up to 1 µM based on the absorbance of PE at 565 nM. The SA-PE*AF647 complex was then incubated with sixfold molar excess of either biotinylated C5a peptidase or free biotin for 30 min at room temperature. In some experiments, the SA-PE*AF647 tetramer was then purified on a Sephacryl S-300 size exclusion column and brought to a concentration of 1 µM based on the absorbance of PE at 565 nM.

Tetramer enrichment. The spleen and inguinal, axillary, brachial, cervical, mesenteric, and LNs were harvested into PBS for each mouse analyzed. In experiments examining the proliferation and differentiation of OVA-specific cells, tissues were minced in collagenase and EDTA as previously described (Pape et al., 2011) to increase the number of antibody-secreting cells recovered. Collagenase and EDTA were not used in the GPI experiments, and collagenase was specifically excluded in some experiments to prevent cleavage of CD23.

A single-cell suspension was prepared and resuspended to 200 µl in Fc block (2.4G2, 2% rat serum, and 0.1% sodium azide). PE*AF647-conjugated nonspecific tetramer was added at a concentration of 5–10 nM and incubated at room temperature for 10 min. PE-conjugated tetramer was added at a concentration of 5 nM and incubated on ice for 30 min, followed by a wash in 15 ml of ice-cold sorter buffer (PBS + 2% fetal bovine serum and 0.1% sodium azide). Tetramer-stained cells were then resuspended to a volume of 200 µl of sorter buffer, mixed with 25–50 µl anti-PE–conjugated magnetic microbeads (Miltenyi Biotec) and incubated on ice for 30 min, followed by one wash with 15 ml of sorter buffer. In experiments where SP and LN single-cell suspensions were divided into 1/2 and 1/4 mouse equivalents before tetramer labeling/enrichment, the volumes were scaled down appropriately. The cells were then resuspended in 3 ml of sorter buffer and passed over a magnetized LS column (Miltenyi Biotec). In some experiments, samples were filled to 3 ml of sorter buffer without a wash step after bead labeling. After sample was run, the column was washed with 3 ml of sorter buffer twice, and then removed from the magnetic field. Pushing 5 ml of sorter buffer through the column with a plunger eluted the bound cells.

Flow cytometry and cell counts. After centrifugation, cell pellets from the enriched and column flow-through fractions were resuspended to 100 µl and 2 ml, respectively, with sorter buffer, and 5 µl was removed for cell counting. Cell suspensions were incubated with surface antibodies for 25 min on ice and washed with sorter buffer. Surface antibodies, used in various combinations, were as follows: FITC-, AF647-, or Biotin-labeled GL7 (BD or eBioscience); AF700- or Pacific blue–labeled anti-CD38 (eBioscience or BioLegend), V500- or eF450-labeled anti-B220 (BD or eBioscience); AF700- or eF605NC-labeled anti-CD19 (eBioscience); eF450-labeled anti-CD21/35 (eBioscience); FITC-, PE-Cy7-, or Biotin-labeled anti-CD23 (eBioscience); eF605NC-labeled anti-CD24 (eBioscience); Biotin-labeled anti-CD40 (eBioscience); FITC-labeled anti-CD43 (clone S7; BD); AF700-labeled anti-CD44 (eBioscience); PerCP-Cy5.5-labeled anti-CD80 (BioLegend); APC-labeled anti-CD86 (eBioscience); eF605NC-labeled anti-CD93 (clone AA4.1; eBioscience), FITC-labeled anti-CD95 (eBioscience); FITC-labeled Igβ (CD79b; BioLegend); AMCA- or PE-Cy7–labeled anti-IgM (Jackson ImmunoResearch Laboratories or eBioscience); PerCP-Cy5.5– or eF450-labeled anti-IgD (BioLegend or eBioscience); APC-labeled anti-IgG1 (BD); and APC-eF780–labeled anti-CD11c, anti-CD4, anti-CD8, anti-Thy1.2, anti-F4/80, and anti-Gr-1 (eBioscience). In some experiments where biotin-labeled antibodies were used, cells were then stained with FITC-, eF605NC or PE-Cy7-labeled streptavidin (eBioscience) for 15 min on ice and washed with sorter buffer. In experiments where cell fixation was not required, cells were resuspended in 0.02 µg/ml DAPI (Sigma-Aldrich) and $DAPI^+$ cells excluded from analysis.

For intracellular staining, pelleted samples were resuspended in 250 µl Cytofix/Cytoperm (BD) for 25 min on ice and washed in permeabilization buffer (BD) before labeling with AF350-conjugated goat anti–mouse Ig H+L (Jackson ImmunoResearch Laboratories) for 30 min on ice and being washed with permeabilization buffer.

Flow cytometry was performed on a 4-laser (355 nm, 405 nm, 488 nm, and 633 nm) or 5-laser (355 nm, 405 nm, 488 nm, 561 nm, and d640 nm) LSR II device (BD) and analyzed with FlowJo software (Tree Star). Fluorescent AccuCheck counting beads (Invitrogen) were used to calculate total numbers of live lymphocytes in the column-bound and flow-through suspensions, as previously described (Pape et al., 2011). Samples collected after OVA injection or KRN adoptive transfer often had a significant number of tetramer-specific B cells that were not retained by the column. When this occurred, the number of tetramer-specific cells in the column flow through fraction was included in the total number of cells.

Enrichment-based affinity measurements. For OVA and GPI affinity assays, spleen and LNs from 4 mice were pooled and split equally into 8 tubes. Samples were resuspended to 100 µl in Fc block containing the appropriate concentration of monomeric antigen or APC-conjugated tetramer and incubated at room temperature for 20 min before labeling with tetramers at the concentrations noted in Tetramer enrichment. For each experiment, the number of cells recovered was shown as a percentage of the number of cells detected in a sample in which no monomeric antigen was added.

MD4 affinity assays were conducted similarly, except that a PE*AF647 tetramer was not used and, splenocytes from MD4 *Rag1*$^{-/-}$ mice containing ~16,000 HEL were mixed with spleen and LNs from 4 WT mice before dividing the sample and incubating with antigen. IC_{50} values were generated using nonlinear regression analysis in Prism (GraphPad Software, Inc.).

Adoptive transfer experiments. For experiments analyzing the function of OVA-specific B cells, purified naive B cells were prepared from spleen and lymph nodes using a B cell negative selection kit from Miltenyi Biotec. The B cells were washed in EHAA medium, adjusted to a final concentration of 5×10^7 cells/ml in pre-warmed EHAA medium, and incubated with 5 µM CFSE (Molecular Probes) for 10 min at 37°C before they were injected intravenously into *Rag1*$^{-/-}$ mice. On the same day, some *Rag1*$^{-/-}$ recipient mice received splenocytes from OTII *Rag1*$^{-/-}$ or DO11 *Rag2*$^{-/-}$ animals containing 10^4 OVA-specific $CD4^+$ helper T cells and 50 µl of 110 µM

of OVA or 27.5 μM of OVA tetramer emulsified in CFA (Sigma-Aldrich) s.c. in the base of the tail.

For experiments analyzing the function of GPI-specific B cells, 10^4 $CD44^{LO}$ $CD25^-$ $CD4^+$ KRN GPI-specific T cells purified by negative selection (CD4 negative selection kit; Miltenyi Biotec; supplemented with anti-CD25 biotin and anti-CD44 biotin) were adoptively transferred into B6.I-$A^{b/g7}$ *Tcra*$^{-/-}$ recipients. In other experiments 2–5 × 10^4 GPI PE tetramer$^+$ Biotin Tetramer$^-$ or C5a PE*AF647 Tetramer$^+$ B cells (B220$^+$ CD11c$^-$ Thy1.2$^-$ F4/80$^-$ Gr-1$^-$ Ter-119$^-$) from B6.I-$A^{b/g7}$ *Tcra*$^{-/-}$ mice were purified at the University of Minnesota Flow Cytometry Core using a 3-laser (407 nm, 488 nm, and 633 nm) FACSAria (BD) and adoptively transferred into NOD *Rag1*$^{-/-}$ *IL2rγ*$^{-/-}$ recipient mice 1 d before the adoptive transfer of 2.5 × 10^4 $CD44^{LO}$ $CD25^-$ $CD4^+$ KRN GPI-specific T cells.

In vitro stimulation. B cells were purified and labeled with CFSE as described in the previous section. Cells were adjusted to a concentration of 2 × 10^6 cells/ml in EHAA (Invitrogen) containing 10% fetal bovine serum (Thermo Fisher Scientific), 100 U/ml penicillin (Invitrogen), 100 μg/ml streptomycin, 2 mM L-glutamine (Invitrogen), 20 μg/ml gentamicin (Invitrogen), and 27.5 μM 2-mercaptoethanol (Sigma-Aldrich). 5 ml of cells were added per well of a 6-well, flat-bottomed plate (and cells were cultured in the presence or absence of 5 μg/ml $F(ab')_2$ goat anti–mouse IgM (Jackson ImmunoResearch Laboratories) and 1 μg/ml anti-CD40 (eBioscience) and incubated for 72 h at 37°C. After incubation, three replicate wells were pooled and enriched using tetramers. DAPI was used to exclude dead cells.

Arthritis clinical index scoring. Total Arthritis Clinical Index Score was determined as previously described (Monach et al., 2008). In brief, each paw was assigned a score 0–3 based on ankle swelling measured with Quick-Mini Series 700 comparator (Mitutoyo U.S.A.) and erythema. The scores from all four paws were totaled for display.

Serum antibody measurement. For anti-OVA antibody measurement, serum was collected 9–10 d after s.c. injection of animals with 50 μl of 110 μM of OVA in CFA, diluted 1–100, and measured for total Ig by ELISA using purified OVA and anti–mouse Ig. Optical density at 405 nM is displayed.

For anti-GPI IgG1 antibody measurement, serum was collected on specified days, diluted 1–900, and measured for anti-GPI IgG1 antibodies by ELISA using recombinant mouse GPI together with anti–mouse IgG1 (BD). Optical density at 405 nM is displayed.

Statistical analysis. All p-values were determined by an unpaired two-tailed Student's *t* test using Prism.

We thank J. Walter, R. Speier, W. Lam, and L. Kalekar for technical assistance; K. Pape and M. Pepper for reviewing the manuscript; T. Martin, P. Champoux, and N. Shah for flow cytometry assistance, and all members of the Mueller and Jenkins Laboratories for helpful discussions.

This work was supported by grants from the Lupus Foundation of Minnesota (D.L. Mueller), the ACR Research and Education Foundation *Within Our Reach* Campaign (D.L. Mueller), the Irvington Fellowship Program of the Cancer Research Institute (J.J. Taylor), and the National Institutes of Health (R01 AI80764 to D.L. Mueller), P01 AI35296 to D.L. Mueller and M.K. Jenkins, R01 AI036914 to M.K. Jenkins, R37 AI027998 to M.K. Jenkins, T32 CA009138 to J.J. Taylor, and F32 AI091033 to J.J. Taylor).

Submitted: 25 October 2011
Accepted: 28 August 2012

REFERENCES

Abbas, A.K., J. Lohr, and B. Knoechel. 2007. Balancing autoaggressive and protective T cell responses. *J. Autoimmun.* 28:59–61. http://dx.doi.org/10.1016/j.jaut.2007.02.002

Adelstein, S., H. Pritchard-Briscoe, T.A. Anderson, J. Crosbie, G. Gammon, R.H. Loblay, A. Basten, and C.C. Goodnow. 1991. Induction of self-tolerance in T cells but not B cells of transgenic mice expressing little self-antigen. *Science.* 251:1223–1225. http://dx.doi.org/10.1126/science.1900950

Barnden, M.J., J. Allison, W.R. Heath, and F.R. Carbone. 1998. Defective TCR expression in transgenic mice constructed using cDNA-based alpha- and beta-chain genes under the control of heterologous regulatory elements. *Immunol. Cell Biol.* 76:34–40. http://dx.doi.org/10.1046/j.1440-1711.1998.00709.x

Borrero, M., and S.H. Clarke. 2002. Low-affinity anti-Smith antigen B cells are regulated by anergy as opposed to developmental arrest or differentiation to B-1. *J. Immunol.* 168:13–21.

Cambier, J.C., S.B. Gauld, K.T. Merrell, and B.J. Vilen. 2007. B-cell anergy: from transgenic models to naturally occurring anergic B cells? *Nat. Rev. Immunol.* 7:633–643. http://dx.doi.org/10.1038/nri2133

Cohen, S.B., P. Emery, M.W. Greenwald, M. Dougados, R.A. Furie, M.C. Genovese, E.C. Keystone, J.E. Loveless, G.R. Burmester, M.W. Cravets, et al; REFLEX Trial Group. 2006. Rituximab for rheumatoid arthritis refractory to anti-tumor necrosis factor therapy: Results of a multicenter, randomized, double-blind, placebo-controlled, phase III trial evaluating primary efficacy and safety at twenty-four weeks. *Arthritis Rheum.* 54:2793–2806. http://dx.doi.org/10.1002/art.22025

Duty, J.A., P. Szodoray, N.Y. Zheng, K.A. Koelsch, Q. Zhang, M. Swiatkowski, M. Mathias, L. Garman, C. Helms, B. Nakken, et al. 2009. Functional anergy in a subpopulation of naive B cells from healthy humans that express autoreactive immunoglobulin receptors. *J. Exp. Med.* 206:139–151. http://dx.doi.org/10.1084/jem.20080611

Fang, W., B.C. Weintraub, B. Dunlap, P. Garside, K.A. Pape, M.K. Jenkins, C.C. Goodnow, D.L. Mueller, and T.W. Behrens. 1998. Self-reactive B lymphocytes overexpressing Bcl-xL escape negative selection and are tolerized by clonal anergy and receptor editing. *Immunity.* 9:35–45. http://dx.doi.org/10.1016/S1074-7613(00)80586-5

Gay, D., T. Saunders, S. Camper, and M. Weigert. 1993. Receptor editing: an approach by autoreactive B cells to escape tolerance. *J. Exp. Med.* 177:999–1008. http://dx.doi.org/10.1084/jem.177.4.999

Goodnow, C.C., J. Crosbie, S. Adelstein, T.B. Lavoie, S.J. Smith-Gill, R.A. Brink, H. Pritchard-Briscoe, J.S. Wotherspoon, R.H. Loblay, K. Raphael, et al. 1988. Altered immunoglobulin expression and functional silencing of self-reactive B lymphocytes in transgenic mice. *Nature.* 334:676–682. http://dx.doi.org/10.1038/334676a0

Hartley, S.B., J. Crosbie, R. Brink, A.B. Kantor, A. Basten, and C.C. Goodnow. 1991. Elimination from peripheral lymphoid tissues of self-reactive B lymphocytes recognizing membrane-bound antigens. *Nature.* 353:765–769. http://dx.doi.org/10.1038/353765a0

Huang, H., J.F. Kearney, M.J. Grusby, C. Benoist, and D. Mathis. 2006. Induction of tolerance in arthritogenic B cells with receptors of differing affinity for self-antigen. *Proc. Natl. Acad. Sci. USA.* 103:3734–3739. http://dx.doi.org/10.1073/pnas.0600214103

Korganow, A.S., H. Ji, S. Mangialaio, V. Duchatelle, R. Pelanda, T. Martin, C. Degott, H. Kikutani, K. Rajewsky, J.L. Pasquali, et al. 1999. From systemic T cell self-reactivity to organ-specific autoimmune disease via immunoglobulins. *Immunity.* 10:451–461. http://dx.doi.org/10.1016/S1074-7613(00)80045-X

Kouskoff, V., A.S. Korganow, V. Duchatelle, C. Degott, C. Benoist, and D. Mathis. 1996. Organ-specific disease provoked by systemic autoimmunity. *Cell.* 87:811–822. http://dx.doi.org/10.1016/S0092-8674(00)81989-3

Lavoie, T.B., W.N. Drohan, and S.J. Smith-Gill. 1992. Experimental analysis by site-directed mutagenesis of somatic mutation effects on affinity and fine specificity in antibodies specific for lysozyme. *J. Immunol.* 148:503–513.

Lohr, J., B. Knoechel, E.C. Kahn, and A.K. Abbas. 2004. Role of B7 in T cell tolerance. *J. Immunol.* 173:5028–5035.

Maccioni, M., G. Zeder-Lutz, H. Huang, C. Ebel, P. Gerber, J. Hergueux, P. Marchal, V. Duchatelle, C. Degott, M. van Regenmortel, et al. 2002. Arthritogenic monoclonal antibodies from K/BxN mice. *J. Exp. Med.* 195:1071–1077. http://dx.doi.org/10.1084/jem.20011941

Mandik-Nayak, L., N. Ridge, M. Fields, A.Y. Park, and J. Erikson. 2008. Role of B cells in systemic lupus erythematosus and rheumatoid arthritis. *Curr. Opin. Immunol.* 20:639–645. http://dx.doi.org/10.1016/j.coi.2008.08.003

Martinez, R.J., N. Zhang, S.R. Thomas, S.L. Nandiwada, M.K. Jenkins, B.A. Binstadt, and D.L. Mueller. 2012. Arthritogenic self-reactive CD4+ T cells acquire an FR4hiCD73hi anergic state in the presence of Foxp3+ regulatory T cells. *J. Immunol.* 188:170–181. http://dx.doi.org/10.4049/jimmunol.1101311

Matsumoto, I., A. Staub, C. Benoist, and D. Mathis. 1999. Arthritis provoked by linked T and B cell recognition of a glycolytic enzyme. *Science.* 286:1732–1735. http://dx.doi.org/10.1126/science.286.5445.1732

Matsumoto, I., M. Maccioni, D.M. Lee, M. Maurice, B. Simmons, M. Brenner, D. Mathis, and C. Benoist. 2002. How antibodies to a ubiquitous cytoplasmic enzyme may provoke joint-specific autoimmune disease. *Nat. Immunol.* 3:360–365. http://dx.doi.org/10.1038/ni772

Meffre, E., and H. Wardemann. 2008. B-cell tolerance checkpoints in health and autoimmunity. *Curr. Opin. Immunol.* 20:632–638. http://dx.doi.org/10.1016/j.coi.2008.09.001

Merrell, K.T., R.J. Benschop, S.B. Gauld, K. Aviszus, D. Decote-Ricardo, L.J. Wysocki, and J.C. Cambier. 2006. Identification of anergic B cells within a wild-type repertoire. *Immunity.* 25:953–962. http://dx.doi.org/10.1016/j.immuni.2006.10.017

Mombaerts, P., J. Iacomini, R.S. Johnson, K. Herrup, S. Tonegawa, and V.E. Papaioannou. 1992. RAG-1-deficient mice have no mature B and T lymphocytes. *Cell.* 68:869–877. http://dx.doi.org/10.1016/0092-8674(92)90030-G

Monach, P.A., D. Mathis, and C. Benoist. 2008. The K/BxN arthritis model. *Curr Protoc Immunol.* Chapter 15:Unit 15 22.

Moon, J.J., P. Dash, T.H. Oguin III, J.L. McClaren, H.H. Chu, P.G. Thomas, and M.K. Jenkins. 2011. Quantitative impact of thymic selection on Foxp3+ and Foxp3- subsets of self-peptide/MHC class II-specific CD4+ T cells. *Proc. Natl. Acad. Sci. USA.* 108:14602–14607. http://dx.doi.org/10.1073/pnas.1109806108

Nemazee, D.A., and K. Bürki. 1989. Clonal deletion of B lymphocytes in a transgenic mouse bearing anti-MHC class I antibody genes. *Nature.* 337:562–566. http://dx.doi.org/10.1038/337562a0

Pape, K.A., J.J. Taylor, R.W. Maul, P.J. Gearhart, and M.K. Jenkins. 2011. Different B cell populations mediate early and late memory during an endogenous immune response. *Science.* 331:1203–1207. http://dx.doi.org/10.1126/science.1201730

Quách, T.D., N. Manjarrez-Orduño, D.G. Adlowitz, L. Silver, H. Yang, C. Wei, E.C. Milner, and I. Sanz. 2011. Anergic responses characterize a large fraction of human autoreactive naive B cells expressing low levels of surface IgM. *J. Immunol.* 186:4640–4648. http://dx.doi.org/10.4049/jimmunol.1001946

Seo, S.J., M.L. Fields, J.L. Buckler, A.J. Reed, L. Mandik-Nayak, S.A. Nish, R.J. Noelle, L.A. Turka, F.D. Finkelman, A.J. Caton, and J. Erikson. 2002. The impact of T helper and T regulatory cells on the regulation of anti-double-stranded DNA B cells. *Immunity.* 16:535–546. http://dx.doi.org/10.1016/S1074-7613(02)00298-4

Shlomchik, M.J. 2008. Sites and stages of autoreactive B cell activation and regulation. *Immunity.* 28:18–28. http://dx.doi.org/10.1016/j.immuni.2007.12.004

Tiegs, S.L., D.M. Russell, and D. Nemazee. 1993. Receptor editing in self-reactive bone marrow B cells. *J. Exp. Med.* 177:1009–1020. http://dx.doi.org/10.1084/jem.177.4.1009

Wang, H., and M.J. Shlomchik. 1997. High affinity rheumatoid factor transgenic B cells are eliminated in normal mice. *J. Immunol.* 159:1125–1134.